

A synchronized Remote sensing monitoring approach in the Livingstone island region of Antarctica

Temenuzhka Spasova ^{*a}, Daniela Avetisyan ^a

^aSpace Research and Technology Institute at the Bulgarian Academy of Science (SRTI-BAS),
Bulgaria
Acad. G. Bonchev Str., bl.1, Sofia 1113, Bulgaria, Tel. +35929883503;

ABSTRACT

Abstract: Data-driven innovations bring significant benefits to societies directly affected by global warming, as they underpin Global and European climate change policy. The application of a synchronous approach and interoperability of data from different sources for environmental monitoring in one of the most vulnerable to climate change regions in the World is the aim of this research. The research was conducted at Hannah Point peninsula, near the Bulgarian Antarctic base "St. Kliment Ohridski" on Livingstone Island, South Shetland Islands, Antarctica. The study area has high ecological importance for tracking the dynamics of processes not only on a local but also on a global scale. Various research sites with different groups of objects serving as environmental benchmarks were selected to be studied. The study objects include snow cover, wet snow, water, ice (including sea ice), herbaceous vegetation, lichens, mosses, soils, and sand. For each of the objects, ground GPS points were defined and in situ spectrometric measurements were performed. Data from an innovative automatic recording weather station (AWG), as well as various indicators and indices based on the spectral reflectance characteristics of the investigated objects in the optical and microwave range, were used. For their generation were used satellite images from Sentinel-1 and Sentinel-2 sensors of European Space Agency. Multiple optical indices were used to demonstrate the changes in the state of the objects for the summer season of 2022-2023. The data obtained and models used will serve the Bulgarian initiative for the construction of the Digital Twins, which is being on pilot developed in the Department of Aerospace Information (SRTI-BAS) and could be used by a wide range of scientists in the field of polar research as well as for climate change education. Open Data were used in this study, to promote the Open science policy and FAIR principles as much as possible.

Keywords: Polar Regions, Climate changes, Destin Earth Antarctica, Spectral reflectance, Interoperability, SAR and optical indices

1. INTRODUCTION

An important problem in the complex approach is synchronisation. Generally, in terms of synchrony, the complex aerospace experiment for remote Earth observation can be subdivided into synchronous, quasi-synchronous, and asynchronous¹. Several criteria determine the degree of synchronisation of an experiment. One of them considers as synchronous all experiments, during which all ground-based measurements are performed on the day X of aerospace image acquisition in the period $t \pm \Delta t$, where t is the moment of space imaging and Δt is the permissible insynchrony between spacecraft and ground measurement complexes¹. Quasi-synchronous measurements are those performed at the same time interval, but not on the day X of the aerospace imaging, but over several days ($\pm \Delta X$) before and after the day X. Asynchronous experiment is when all the work is performed at any time of a day, in which one or more synchronous or quasi-synchronous experiments are made. The values of Δt and ΔX are not constant and depend on the nature of the subjects studied and the conditions of measurements¹. In general, the slower the physical parameters are measured, the more the experiment can be considered 'more synchronous' and vice versa¹. The complex synchronous remote sensing aerospace experiment is most effective when conducted from three levels: spacecraft; airplanes, helicopters, or unmanned aerial vehicles (drons); ground measuring complexes².

[*tspasova@space.bas.bg](mailto:tspasova@space.bas.bg); <http://www.space.bas.bg/en/structure/department/asi.html>

The synchronous aerospace experiment for remote exploration of the Earth has some characteristic features, the most important of which are: it takes place in a time interval when the Sun is at its zenith; due to the high speeds of airplanes, helicopters, and especially spacecraft movement, the duration of the experiment is very short - up to a few minutes; due to variety and complexity of parameters and conditions under which they are carried out, each experiment is unique and practically unrepeatable². Thus, the experiment made under the Antarctic conditions is, in itself, relevant and unique in time and place for the area of Livingstone Island. It can be assumed that the approach is synchronous, since the most dynamic surface for the specific area is the sea water and wet snow, and in the studied area of Hannah Point do not have significant changes in the state of the objects for the dates of the experiments. The field studies were also carried out on the same dates during the 31st Bulgarian Antarctic expedition.

Despite the systematic and intensive, multi-year, diverse glaciological studies in the polar regions, to overcome their partial, still fragmentary nature and to implement the modern concepts, interdisciplinary and complementary studies are needed^{3,4}. The present research aimed to create a methodology for ecological monitoring in polar latitudes applying a complex synchronous approach and interoperability of data.

The Polar Regions are distinguished by unique conditions, influencing in specific way processes occurring in ecosystems. The theoretical and experimental basis for some combinations of conditions is multivariate and/or partially ambiguous. The reason lies in the non-linear dependencies of the "melting/freezing" process of water on indirectly related governing parameters, which define narrow transition regions between relatively stable states of its phase space^{3,4}. The depicted processes are complex. Their study is a challenging task that needs to utilize the whole potential of the available technologies to be solved. In our study, we test the ability of remote sensing technology for monitoring and assessment of processes influenced by climate change and global warming combining the advantages of field measurements for validation purposes. Creating a rich database with spectral information of different objects will facilitate further monitoring using satellite remote sensing technology.

However, the frequent and dense cloud cover over the study area is a limitation for obtaining qualitative and continuous data for satellite remote sensing using optical imagery only. The application of combined approaches and data (in this case SAR and field measurement data) enables differentiation of various objects and highlights locations where a natural component or object is present or not. The lack of continuous cloud-free Sentinel-2 time series for the Antarctic area is compensated by the sufficiently good temporal and spatial resolution of Sentinel-1A SAR data. The availability of ground-based data in addition allows effective and cost-effective monitoring of climate change in remote areas using SAR data. The SAR C-band enables the effective study of various objects⁵⁻¹⁵ and especially wet snow and ice^{3,4,16-19}. Using SAR data, we studied the type of changes in the digital value of the reflected signal (Q) from various objects, including water in different phase states. For the study of vegetation^{20-24,26,27} (herbaceous sp., lichens, and mosses), water^{16,25} (in all aggregate states), and soils^{26,27}, numerous optical indices have been used to demonstrate the changes occurring in them. Most of the indices are developed to monitor vegetation but they could also be informative for detecting changes in other types of objects, especially in their transition stages. These conditions can be observed and evaluated remotely utilizing the Disturbance Index (DI)^{28,29}, Modified Chlorophyll Absorption Ratio Index (MCARI2), Modified Soil-Adjusted Vegetation Index (MSAVI2), Normalized Difference Vegetation Index (NDVI), Normalized Differential Greenness Index (NDGI), Normalized Difference Water Index (NDWI), and Moisture Stress Index (MSI).

The application of a synchronous approach and utilization of data from different gave us valuable information for the processes taking place on Hannah Point peninsula, Livingstone Island, Antarctica in the summer season of 2022-2023. The experiment, methodology used and results obtained are reported in the present research paper.

2. STUDY AREA

Declared a nature reserve Cape Hannah is located on the east side of the entrance to Walker Bay and the west side of the entrance to South Bay. The coordinates of Cape Hannah are 62°39'16"S and 60°36'48"W (Figure 1), it is located 13.95 km northeast of Elephant Point, 8.16 km west southwest of Ereby Point, 12.36 km west-southwest of Hesperides Point and 11.76 km northwest of Miers Bluff.

The Hannah Point area is among the most attractive destinations of Antarctic cruise tourism. It offers a spectacular walk past colonies of penguins and seals, cormorants, and petrels. The local climate is typical of the peripheral island territories of Antarctica: wet and windy, cool, with an average air temperature of 1.3°C in the warmest month and -7°C in the coldest. Sunny days are few and rare.

Cape Hannah is home to over 1,500 pairs of Gentoo penguins and 1,000 pairs of Antarctic penguins that nest in the area. In the last few years, several pairs of Macaroni penguins have also been spotted living together with the Antarctic penguin. Large colonies of giant petrels are found on the ridges above the penguin area, as well as many species of gulls and snowy owls. Antarctic cormorants are also common in the area.

Both types of Antarctic flowering plants are widespread: *Colobanthus quitensis* and *Deschampsia Antarctica*³⁰ (Figure 2). The most common lichens are *Ochrolechia frigida* and *Usnea antarctica*, which form huge green, gray, yellow, and reddish carpets. Different types of mosses can also be found. On the territory of Cape Hannah, clearly can be distinguished several green carpets, which favors the development of soils. The most common species throughout Antarctica and Cape Hannah is *Sarconeurum glaciale*³¹ (Figure 2).

In order to comply with all regulations for the protection of the local flora and fauna in the area, visits during the reproductive period of the animal species are prohibited. The allowed presence of people in the reserve is no more than 6 astronomical hours during the daylight hours. Gathering large groups in one place is also not recommended³⁰.

For the conduct of the experiment at Cape Hannah Point, only one person from the team is allowed to be on the ground, which for the large spaces in the Antarctic and the uniformity of the experiments on the sites is absolutely sufficient and economically advantageous.

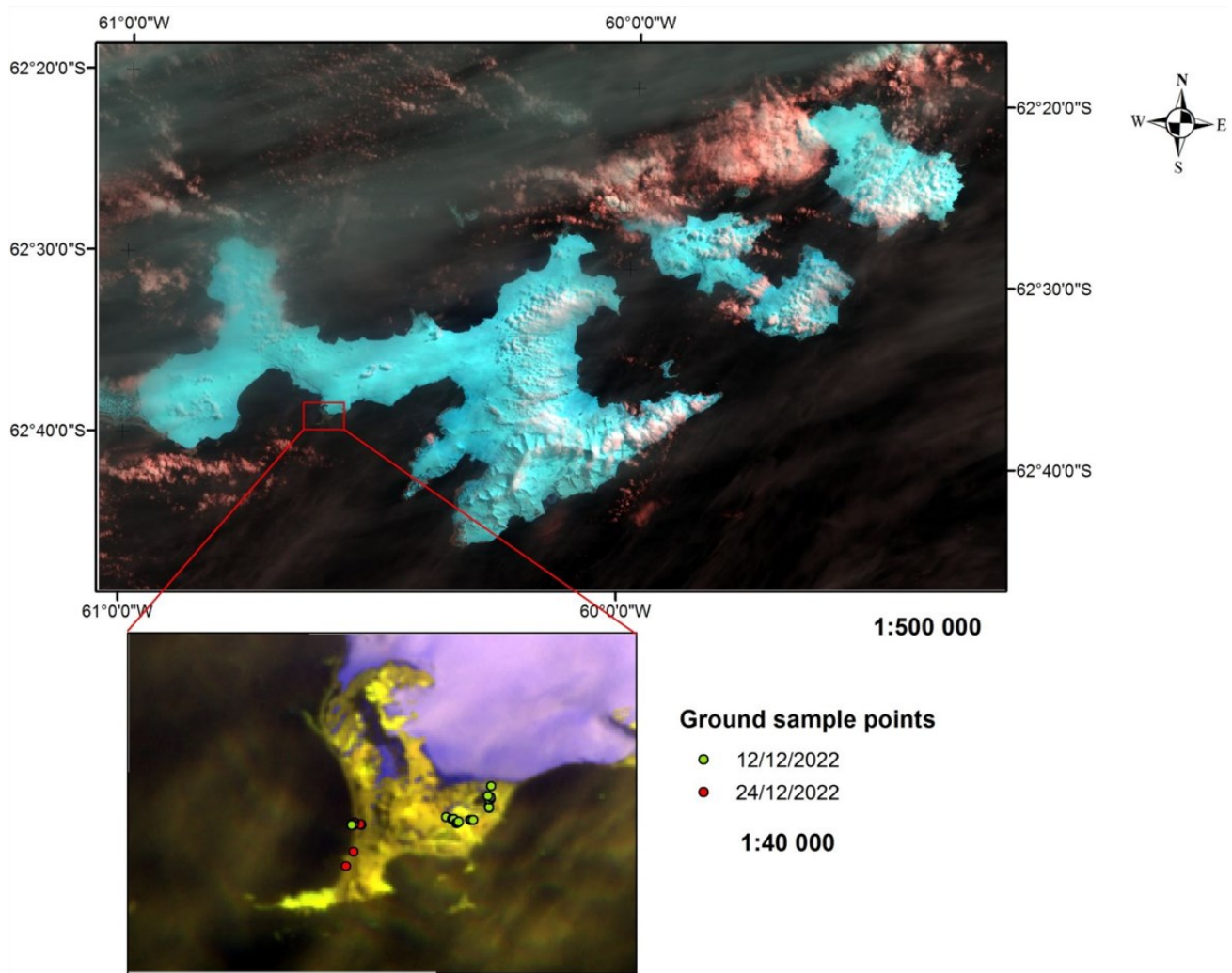


Figure 1 Livingston Island (upper image) and Hannah Point peninsula (bottom images) with the ground sample point locations of the studied objects on Sentinel-2 composite images (Bands 12, 8a, 4 and Bands 12, 11, 2 respectively)^{32,33}



Figure 2 Hannah Point; Autor: Temenuzhka Spasova 31st Bulgarian Antarctic Expedition, 12/12/2022 and 24/12/2022

3. DATA AND METHODS

3.1. Data used

Selection of test areas

In order to verify and validate the proposed methodology, a selection of test areas was first made through visual interpretation and initial revision of satellite images from the Copernicus program. Due to the frequent and dense cloud cover, the selected images shall be of different days to maximise the size of the test area. The test sites should include various objects in different states, which should be located both on the ground and in the sea. In this way, certain territories can be better compared and the indices and classifications made would be more precise. For each image, the so-called area of interest (AOI) has been selected precisely. Each of these areas should be the same for optical and radar images for matching images in subsequent processing or reuse of the information. The selection of the individual studied objects was performed during the field campaign on 12/12/2022 and 24/12/2022, during which Ground Control points of each individual object were generated.

Ground Control points (GCP)

For the purpose of the study, the following Ground Control Point (GCP) locations were generated and applied: 25 GCP, generated on 12/12/2022, and 6 GCP – on 4/12/2022. The points were generated via OruxMap in offline mode and published for Open access on a platform (catalogue) such as open data at www.Destination-earth-antarctica.eu. The generated point locations are freely available on a catalogue page, aiming freely publishing data from the Antarctic polar studies in line with the DCAT-AP data standard³⁴.

Spectrometer data

The field spectral surveys were performed using a spectrometer in the visible range (Sekonic Spectrometer C-800), a full-spectrum color meter that can accurately measure any type of light³⁵. The data from the spectrometer is with the following parameters³⁶: Color temperature, CCT (Correlated Color Temperature), Δuv (Deviation) between the correlated color temperature and the place of emission of the black body, Hue (in degrees), Sat – Saturation is the index to express the intensity or chroma. Using these data, a study of the color characteristics of the objects was conducted. For

each spectral reflectance characteristic (SRC), the color characteristics (color coordinates (x,y) and dominant wavelength) in the spectral range 380-780 nm were calculated relative to CIE 1931 and a standard source of electromagnetic radiation³⁶.

Satellite data

The satellite data used in the study are from the Sentinel-1-A and Sentinel-2-B satellites of the European Space Agency (ESA). Sentinel-1-A is Synthetic Aperture Radar (SAR)³⁷ sensor, and Sentinel-2B is a Multi-Spectral Instrument (MSI)^{32,33} recording data in the optical range with different spectral resolutions. Data by dates and satellites used are represented in Table 1.

Table 1. Satellite images acquisition dates

Satellite	Date	Spectral Band, wavelength	Band	GSD*, m
Sentinel-1-A	29/11/2022 11/12/2022 23/12/2022 16/01/2023	$\lambda=5,6\text{cm}$, Polarization: HH	C	10x10**
Sentinel-2-B	07/12/2023	0.665 μm	4	10
	16/01/2023	0.865 μm	8a	20
		1.61 μm	11	20
		2.19 μm	12	20

*Ground Sample Distance (GSD)** Pixel Spacing Resolution (rg x az)

Automatic recording weather station (AWG) data

Another type of data, which at this stage is part of the catalogue, but still is not involved in the analysis, was derived from the Automatic recording weather station (AWG), presented in detail in Table 2. The data were generated from field surveys on Livingstone Island in December 2022 and provided by Spasova and Avetisyan, Department of Aerospace Information, Space Research and Technology Institute, Bulgarian Academy of Sciences and by Popov and Shirov, OXYMET³⁸.

Table 2. Raw Data from Automatic recording weather station (AWG), an Ecological Magnesium-Air battery (11/12/2022)

Battery Cell 1 Voltage: 1.04
Battery Cell 2 Voltage: 1.80
Battery Cell 3 Voltage: 3.15
Temp.: 49.62F; 9.78C
GPS data W: -62. 64 ; S -60.37 ; GPS date: 0
Auto Weather and GPS logger, code name Alissa;
Powered by: OXYMET - an ecological Magnesium-Air battery;
Design & development by: Iliyan Popov, Boris Shirov ;
Light: 4.96
Battery Cell 1 Voltage: 1.04
Battery Cell 2 Voltage: 2.12
Battery Cell 3 Voltage: 3.13

Temp.: 49.80F; 9.88C
GPS data W: -62.64 ; S -60.37 ; GPS date: 0
Auto Weather and GPS logger, code name Alissa;
Powered by: OXYMET - an ecological Magnesium-Air battery;
Design & development by: Iliyan Popov, Boris Shirov ;
Light: 4.97

Drone data

The last data source is the DJI Mavic 2 drone. The drone photography was used to correctly verify the environment, in which the experiment was made and for the synchronized remote sensing monitoring approach. The Drone images are from the days of field measurements (12/12/2022 and 12/24/2022) (Figure 3, 4).



Figure 3 Hanna Point – 12/12/2022, Drone data; Personal archive, Autor: Temenuzhka Spasova



Figure 4 Hanna Point – 24/12/2022, Drone data; Personal archive, Autor: Temenuzhka Spasova

3.2. Methods

Description of the synchronized experiment

During the experiment, field measurements of the spectral reflectance characteristics (SRC) of the studied objects and drone photography were performed. The timing of the experiment was consistent with the passage of Sentinel-1 and Sentinel-2 satellites over the study area. Due to the distance of Hannah Point from the Bulgarian Antarctic Base (BAB) and availability of logistical support, the field surveys often do not coincide with the optimal weather conditions for satellite remote sensing with optical data. The generation of SRC of the studied objects and the drone photography were performed on 12/12/2022 and 24/12/2022. Unfortunately, the weather conditions were not suitable for satellite remote sensing through optical imagery and the Sentinel-2 images from these dates are with clouds on them. Therefore, we used the Sentinel-2 image acquired on the closest date before the day with ground-based research (7/12/2022). We assume that there weren't significant changes in the onshore sites during these 4-5 days. The reference date for the verification of the dynamics was 16/01/2023. The surveys were carried out within the same time range, which defines them as quasi-synchronous for the optical data. As regards the Synthetic Aperture Radar (SAR) images from the Sentinel-1 sensor, there is sufficient representative data and dates close to the dates with field surveys, such as 11/12/2022, 23/12/2023, 29/11/2022, and 16/01/2023.

Spectrometric measurements and data interpretation

The research aimed to create a methodology for a complex synchronous approach and interoperability in remote sensing in polar latitudes. Through spectrometric measurements of various objects on Hannah Point, Livingston Island, Antarctica, a database of SRC (spectral library) was created. This database was used and is available for the calibration of satellite sensors for remote sensing of various natural objects, for environmental protection, and for the needs of comparative analysis of objects in polar conditions and latitudes. The database will be upgraded and enriched with additional data after future studies.

Colour is a major factor in Remote sensing and a leading characteristic for each of the objects studied. The analysis of the SRC includes a study of the color characteristics of the objects. For each SRC of a given object, color characteristics (color coordinates (x, y) and dominant wavelength in the spectral range 380-780 nm relative to CIE 1931 and a standard source of electromagnetic radiation D₆₅) were obtained³⁶. The color coordinates of rocks, soils, and vegetation can be successfully used for object recognition by spectral data. According to the methodology proposed, only the selected points from the study area were characterized. The final selection of the objects was facilitated by drone photography. In-situ (field) spectrometric measurements of the SRC of the selected objects in their natural conditions were performed. A GPS control point was taken for each of the profiles using OruxMaps. This product works in offline conditions, but it generates enough GPS data and statistics successfully.

The next step of the methodology was the selection of algorithms for the interpretation of the measured spectral data for the recognition of the type of studied objects. A comparative analysis of the obtained library of SRC with reference spectral libraries for the studied objects and those obtained through the Sentinel 2B MSI sensor was made.

Remote sensing uses a wide range of the electromagnetic spectrum - from ultraviolet to radio waves, but the visible, infrared, and microwave regions of the Electromagnetic spectrum (EMS) have the most applications and importance³⁹.

Using the spectrometer, measurements in the visible and a narrow part of the near-infrared range (0.38–0.78) were made. The average height (h) of the spectral profiles taken is ~1m. In the same spectral range, there is also a measurement from the Sentinel 2 sensor (from band 1-0.44 to band 7-0.783). The in-situ measurements were used for validation of the satellite-based optical data.

In the visible range, primary colors with the following wavelengths are distinguished: Violet 0.380–0.440; Blue 0.440–0.490; Green 0.490–0.565; Yellow 0.565–0.595; Orange 0.595–0.620; Red 0.620–0.760^{16,39}.

Another EMS range that has been used in remote sensing for polar latitudes is near- and mid-infrared and in this case 0.7–2.19 μm . In the present study, we analysed the SRC of the objects from 0.70 to 0.78 μm using both the data obtained by a spectrometer and by Sentinel-2 satellite sensor, which is a prerequisite for data comparison and validation.

Each of the spectral ranges has its advantages and disadvantages, which determine the specifics of the measurement technology and the type of tasks to be solved³⁹. Due to a number of advantages, the most widely used spectral ranges for polar studies of objects on the Earth's surface are the visible and near-infrared spectral ranges between 0.4 and 1.3 μm . Of course, there are also disadvantages to using satellite remote sensing for the polar latitudes and they are related to the lighting conditions and the state of the atmosphere. Therefore, in our experiment, we used only satellite data acquired during the summer season.

Classification of satellite optical and radar data

The measured reflectance of satellite sensors depends on the local characteristics of the Earth's surface, which need to be detected to retrieve information from image data. Theoretically, a single spectral band of a remote sensing image must be sufficient to classify objects, but the classification of complex multispectral data produces much better results². Using imaging software, satellite images from different periods, over the same territory of interest, and for each of the profiles studied were processed, classified, and analysed. To study the changes occurring in the individual objects, numerous indices were used. They were based on optical and radar data. The indices for classification optical data are presented with the formulas for their calculation in Table 3.

Table 3 Calculation formulas and description of the optical indices used in the study

Index	Formula	Description
Normalized Difference Vegetation Index (NDVI) ⁴⁰	$\text{NDVI} = (\rho_{783} - \rho_{665}) / (\rho_{783} + \rho_{665}) \quad (1)$	NDVI is the most widely used spectral index for vegetation monitoring and evaluation of the photosynthetic activity. NDVI is strongly correlated with climate variations and can serve as an effective measure of climate-related vegetation changes.

Modified Soil-Adjusted Vegetation Index (MSAVI ₂) ⁴¹	$MSAVI_2 = \frac{2\rho_{783} + 1\sqrt{(2\rho_{783} + 1)^2 - 8(\rho_{783} - \rho_{665})}}{2} \quad (2)$	MSAVI ₂ is an adapted version of the Soil-Adjusted Vegetation Index (SAVI), developed to diminish NDVI inaccuracies in areas with exposed soil surface (Huete, 1988).
Modified Chlorophyll Absorption Ratio Index (MCARI ₂) ⁴²	$MCARI_2 = \frac{1.5[2.5(\rho_{783} - \rho_{665}) - 1.3(\rho_{783} - \rho_{559})]}{\sqrt{(2\rho_{783} + 1)^2 - (6\rho_{783} - 5\sqrt{\rho_{665}}) - 0.5}} \quad (3)$	MCARI ₂ is a modified version of the Chlorophyll Absorption Ratio Index (CARI), developed to estimate chlorophyll variations. The derived MCARI ₂ index is less sensitive to variations in chlorophyll concentration but has a great linear relationship green LAI.
Normalized Difference Water Index (NDWI) ⁴³	$NDWI = (\rho_{865} - \rho_{1375}) / (\rho_{865} + \rho_{1375}) \quad (4)$	NDWI capitalizes on the differential response of the NIR and SWIR reflectance in healthy vegetation, enhancing the precision in assessment of the vegetation moisture content.
Moisture Stress Index (MSI) ⁴⁴	$MSI = \rho_{1610} / \rho_{833} \quad (5)$	MSI is used for vegetation water stress analysis. Higher values of the index indicate for greater plant water stress and consequently, for less moisture content.
Disturbance Index (DI) ²⁸	$nBR - (nGR + nW) \quad (6)$	DI was proven as an effective approach for detecting vegetation disturbance and monitoring its change in terrestrial ecosystems.
Normalized Differential Greenness Index (NDGI) ⁴⁵	$NDGI = \frac{GR_n(t_2) - GR_n(t_1)}{ GR_n(t_2) + GR_n(t_1) } \quad (7)$	NDGI estimates slight positive and negative changes in the vegetation green mass for a given period. NDGI ranges from +1 to -1, as NDGI < 0 indicates a negative change, and NDGI > 0 indicates a positive change.
Normalized Difference Snow Index (NDSI)	$NDSI = \frac{\rho_{490} - \rho_{1610}}{\rho_{490} + \rho_{1610}} \quad (8)$	It is effective for studying the snow cover. Its values range from 0 to 1 (one). The most suitable channels are 2 and 11 of Sentinel 2 MSI ^{46,47} .

In present study, we introduced the Disturbance Index (DI) for monitoring objects with SRC in the environment of Livingston Island. The index is primarily applied for assessment vegetation disturbances and it has shown to be more accurate, compared to the standard spectral indices²⁹. The DI is based on the linear orthogonal transformation of multispectral satellite images - Tasseled Cap Transformation (TCT)^{48,49} and uses unique transformation matrices for each sensor. In present study, we used TCT matrix proposed by⁵⁰ involving all spectral bands of the Sentinel-2 sensor. Utilization of all spectral information increases significantly the degree of identification of the three main components of the Earth's surface - soil, vegetation and moisture⁵¹. The outputs from TCT are multi-band images containing three layers – Wetness (TCW), Brightness (TCB), and Greenness (TCG). After their generation, decomposition on each of them is being applied. The next step is the calculation of the normalized values of the Tasseled cap components, the values of mean and standard deviations. After the normalization, the three component indices were combined linearly to acquire the DI²⁸.

Another index based on the TCT is the NDGI. Before its final calculation, it is needed the variables of the index to be calculated. The formula for calculation of the variables is as follows:

$$GR_n(t) = \frac{GR(t) - E\{GR(t)\}}{St.Dev.[GR(t)]} \quad (9)$$

,where $GR_n(t_1)$ and $GR_n(t_2)$ are the normalized values of the Greenness component at time points t_1 and t_2 ; $|GR_n(t_1)|$ and $|GR_n(t_2)|$ are the absolute values of the same component; $E\{GR(t)\}$ is the mean of $GR(t)$.

And last but not least, optical indices for snow and ice were used in the study. To study the snow cover dynamics, the Normalized Difference Snow Index is calculated and classified, which is extremely accurate in areas with a constant presence of snow and ice (Table 3).

For calculation of the radar coefficients in the complex synchronous approach, the SR between two SAR images from different time points was used. The coefficient is a dimensionless quantity, and the formula is as follows:

$$r(i,j) = \frac{\sigma(i,j)t_1}{\sigma(i,j)t_2} \quad (10)$$

,where σ is the microwave reflectance coefficient for time instant t_1 (satellite image of earlier date) and t_2 for time instant (satellite image of later date), i, j are the row and column numbers of pixels in a given SAR image, and r is the relative soil moisture content reported for the corresponding period between two images of one polarization. This mathematical approach was used between four images over a period of about a month, showing promising results in identifying areas of moderate and high change in vegetation, wet snow, ice, and water¹³. The values above 2 register serious changes in the reflectance of a given object in selected areas, and low values below 1.0 indicate little or no change in an object's reflectance. A threshold value of 2.0 was used to discriminate large changes in reflectance or the presence of a new object¹⁷.

Automatic recording weather station (AWG)

An ecological Air-Magnesium battery was tested for the needs of meteorological independent information in the area. It was used in the Automatic recording weather station (AWG), which is an innovative instrument for measuring and recording ambient temperature, illumination, UV radiation, GPS coordinates, barometric pressure, and altitude. The battery is activated with seawater and can operate for several weeks, with the measured data recorded on a SD memory card. The device is built on the Arduino hardware platform. The equipment is intended for operation at the Bulgarian Antarctic station on Livingston Island, but due to the similar environmental conditions, the data obtained are representative of the entire island ¹¹(Figure 5).



Figure 5 Innovative Automatic recording weather station (AWG)³⁸, Livingston Island. Autor: Temenuzhka Spasova, 2022

4. RESULTS AND DISCUSSION

4.1. SRC of the studied objects

Most detailed SRC of the studied objects was obtained through a spectrometer in the visible range of the electromagnetic spectrum. It can be easily compared and used and this helps us to accumulate a large amount of information about research objects and their interpretation.

The analyses of the color temperature measured by the spectrometer in Kelvin (K) show that at each of the test points, values above 5000K or high K-values (5500 – 6500K) predominate, which correspond to cold, white light (Figure 6,7,8). The average K-values (4000-4200K), defined as 'neutral' light, are absent in the field studies at Hannah Point.

Even objects with similar SRC can be distinguished by indicators such as color temperature and color coordinates, Hue, or Sat - Saturation. A representative example was found at points with very similar values such as P60 and P62 (mosses) (Figure 6), for P52 (wet dark snow) and P65 (ice) (Figure 7). At objects P42 and P49 (Figure 7), very similar values of water and muddy water were also observed, where Δuv (Deviation) between the correlated color temperature and the place of emission of the black body was almost the same, but the Color temperature is with a difference of 1000 K. These indicators values indicate the presence of a different object.

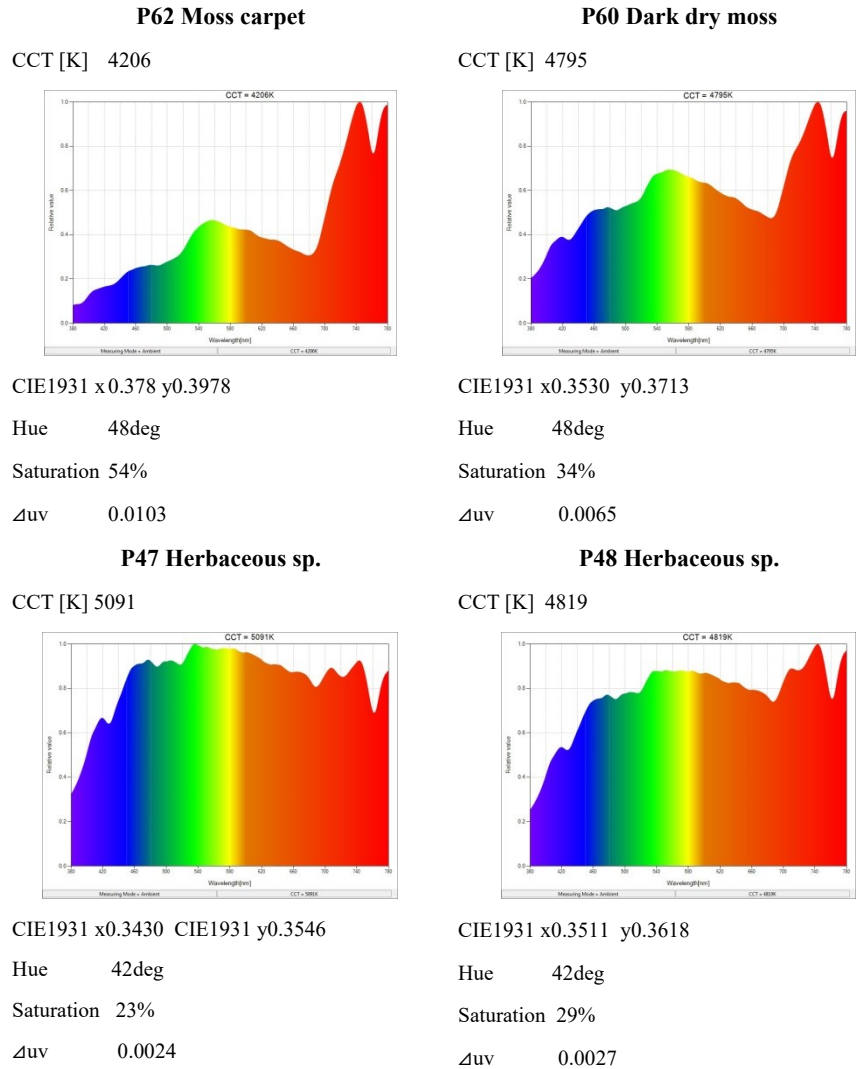
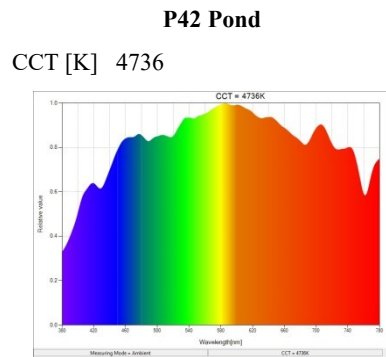
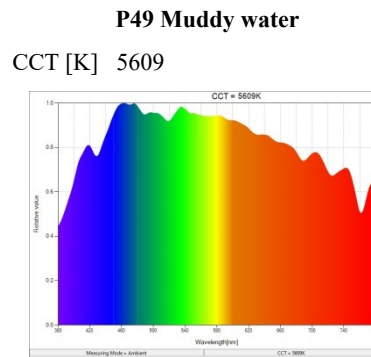


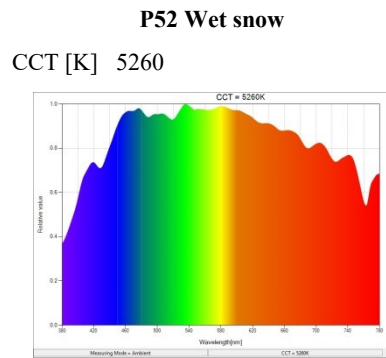
Figure 6 Spectral reflectance characteristics of vegetation obtained by a spectrometer; Hannah Point, Antarctica – 12/12/2022



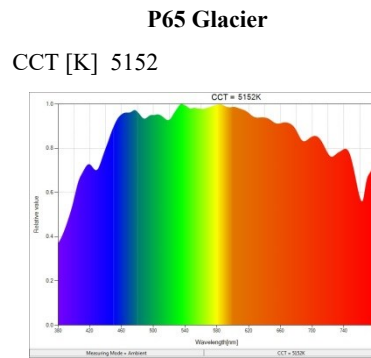
CIE1931 x0.3528 y0.3562
 Hue 37deg
 Saturation 27%
 Δuv -0.0007



CIE1931 x0.3300 y0.3397
 Hue 35deg
 Saturation 11%
 Δuv 0.0004



CIE1931 x0.3383 y0.3472
 Hue 38deg
 Saturation 18%
 Δuv 0.0006



CIE1931 x0.3410 y0.3484
 Hue 37deg
 Saturation 19%
 Δuv 0.0001

Figure 7 Spectral reflectance characteristics of water body, wet snow, and glacier obtained by a spectrometer; Hannh Point, Antarctica
 – 12/12/2022

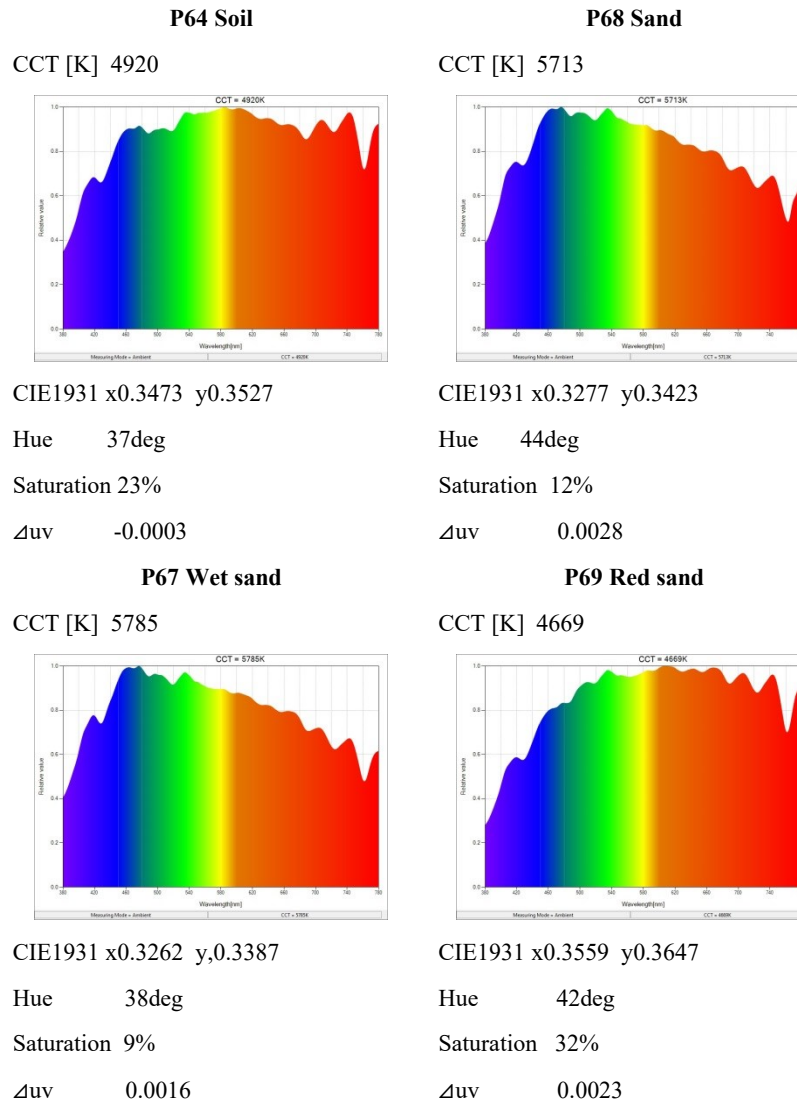


Figure 8 Spectral reflectance characteristics of soil and sand obtained by a spectrometer; Hannh Point, Antarctica – 12/12/2022

Spectral reflection profiles of the objects in the individual sample point location generated on Sentinel-2 composite images are presented in Figures 9, 10 and 11. Among the profiles shown in Figure 11, the typical soil profile is characterised by the highest spectral reflectance (SR) in the visible and NIR areas of the electromagnetic spectrum, and the screes and dry sand have SR less than 0,2. On the other hand, there are no objects in the plant group (Figure 9) with a SR below 0,2. The highest SR values have dark dry moss and the lowest herbaceous vegetation (Figure 9). Mosses have similar SRC to those of soils and rocks, as they develop mainly on such surfaces and have a lower moisture content. The herbaceous vegetation in the study area is developed on soils and under wet conditions and thus has a higher moisture content or lower SR values in the visible and NIR ranges compared to mosses. The SR values of water group objects (Figure 10) vary from less than 0,2 for the typical water profile and 0,3-0,35 for glacier. SR from ice and snow objects clearly differs with higher SR values than water bodies.

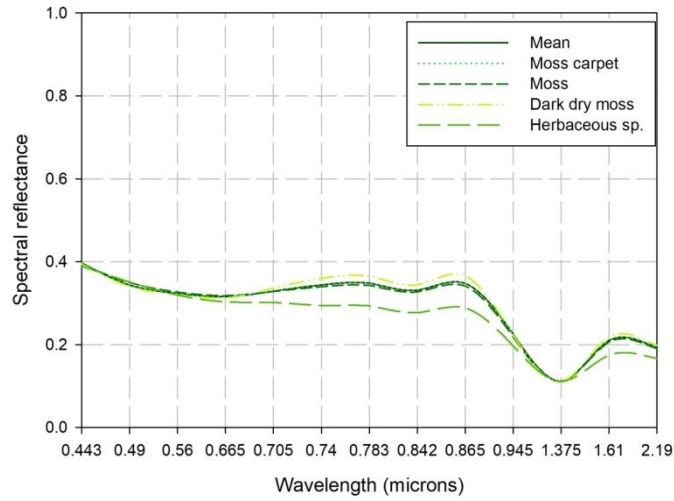


Figure 9 Mean values of the SRC of vegetation generated on Sentinel-2 images (07/12/2022 and 16/01/2023)

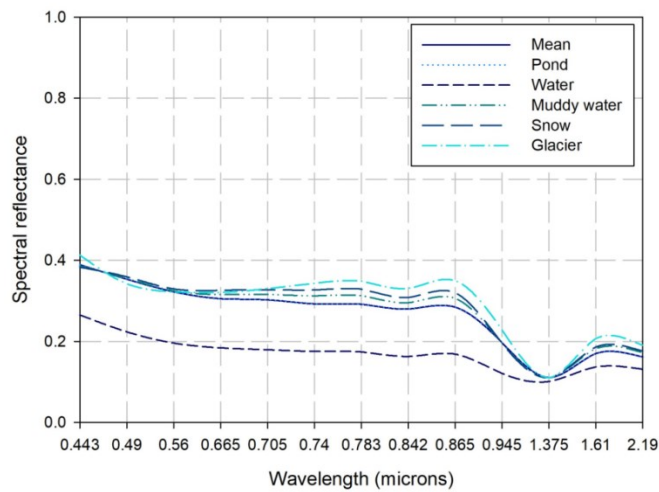


Figure 10 Mean values of the SRC of water bodies, snow, and glacier generated on Sentinel-2 images (07/12/2022 and 16/01/2023)

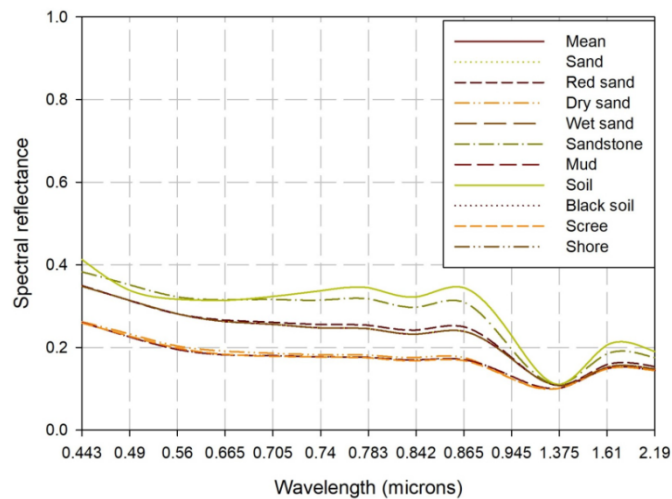


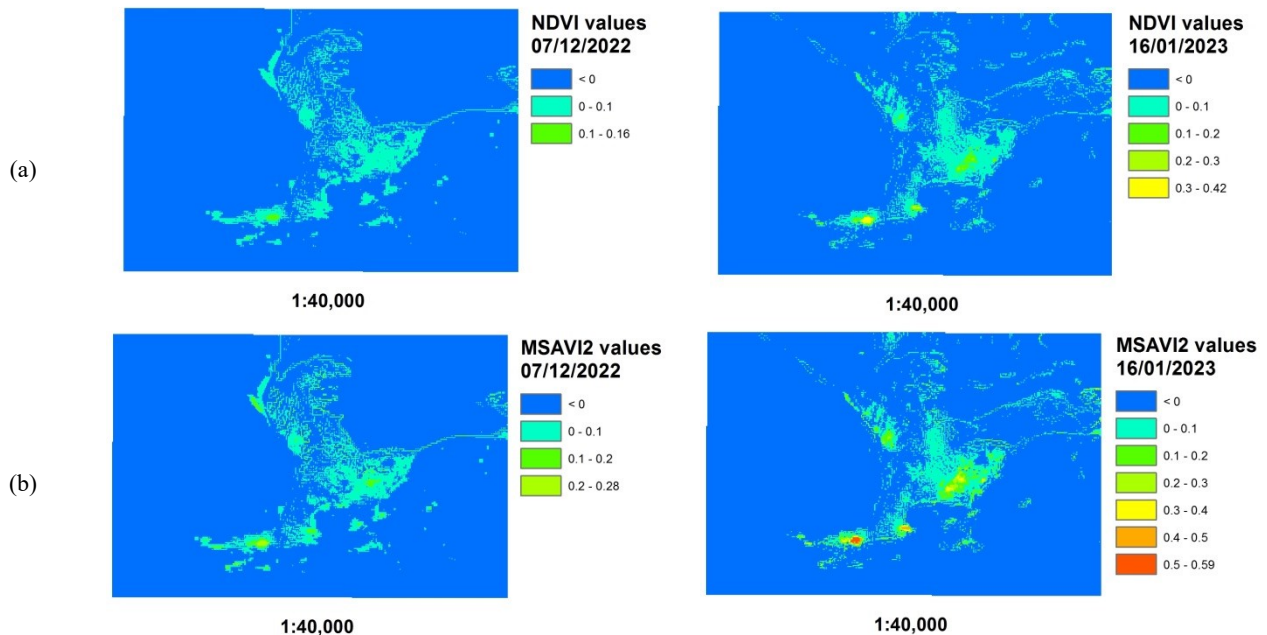
Figure 11 Mean values of the SRC of soil, sand, and rocks generated on Sentinel-2 images (07/12/2022 and 16/01/2023)

4.2. Spectral indices and assessment of their dynamics

Dynamics and territorial distribution of the optical indices values

The spectral indices showed a weaker ability to differentiate the individual objects on the Earth's surface in early December compared to mid-January. The only exception is DI, where the opposite trend was observed (Figure 12d). This is due to the similar SRH of the individual objects, which results in similar values of the spectral indices applied. As the summer progresses and the state change of the studied objects intensifies, their SRCs become more distinct, which also affects the indices values. This is particularly evident in the transition of ice and snow to water and the growth of areas occupied by different types of vegetation. DI and NDWI showed to be superior, amongst the vegetation indices, in the assessment of ice and snow covers dynamics (Figure 12d,12e). DI has not been used so far to evaluate disturbances in snowy/icy areas. From the results obtained, it can be seen that it is distinguished by higher values at the beginning of summer and stabilizes as the season progresses (Figure 12d). MSAVI2 showed to be the most suitable among the vegetation indices applied in the present study to assess the dynamics of terrestrial vegetation. The maximum MSAVI2 values increased by 0.31 in the period between 7/12/2022 and 16/01/2023, and the number of pre-defined indices classes increased from four to seven (Figure 12b). In comparison, the NDVI maximum values increased by 0.26, and the pre-defined classes by two numbers (from three to five) (Figure 12a). MCARI2 has accounted for both terrestrial and aquatic vegetation dynamics (Figure 12c).

For the snow optical index, there was an increasing trend of the areas occupied by snow and wet snow, which is due to the transition period in which its values vary from 0 to 1 (one). Values above 0.80 could be considered when investigating older snow cover and ice. There is no ice presence in the considered study area because the values are below 0.75 (Figure 12f).



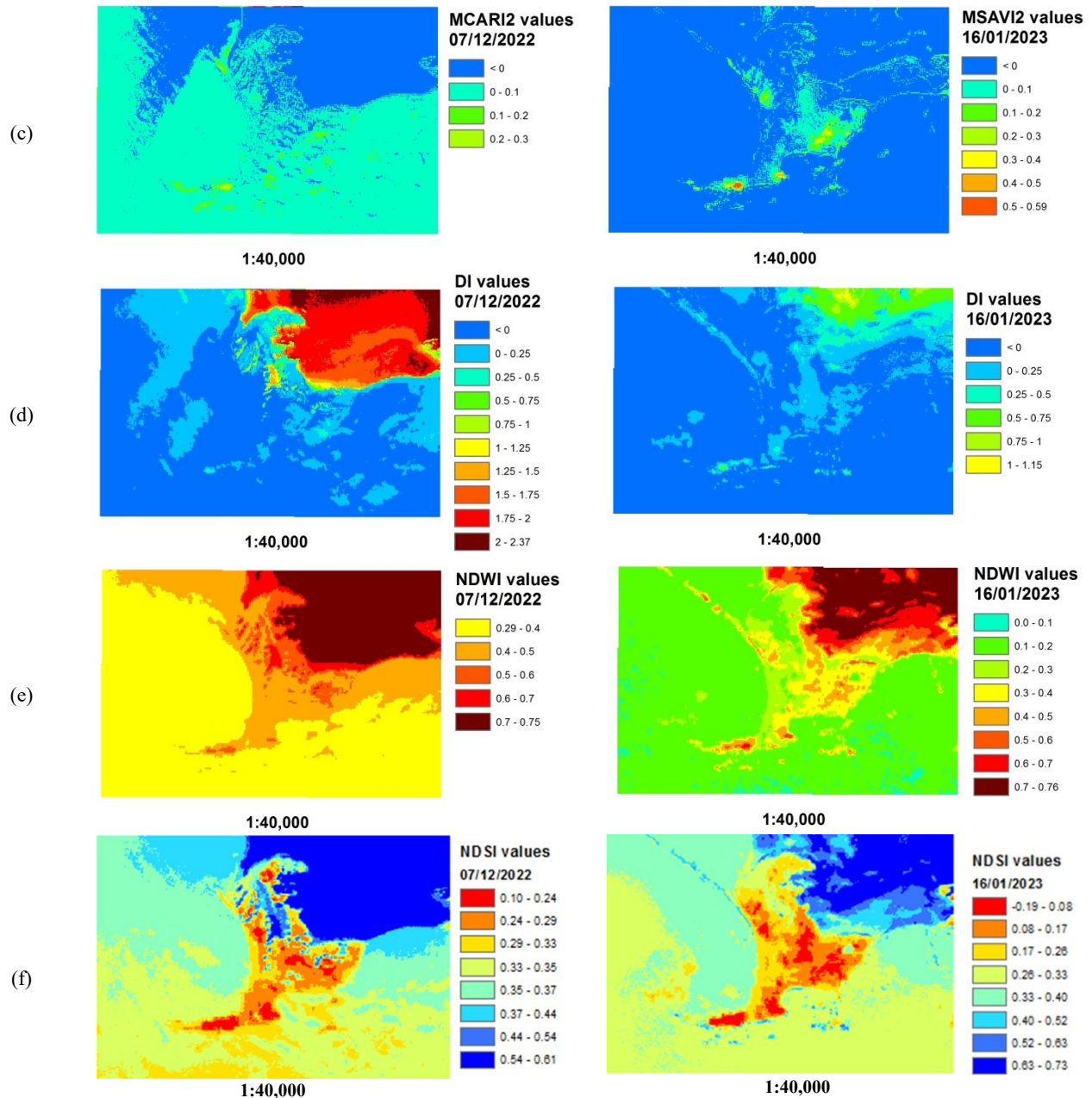


Figure 12 Spatial distribution of the optical indices values throughout the study area

Optical indices values in the locations of sample point objects

The analysis of the Sentinel-2 –based spectral indices calculated for the individual sample point objects showed the highest values for P61 (Moss) for the most of indices (MCARI2, MSAVI2, NDVI, NDWI, MSI) (Table 4). DI had the highest value in P45, which is also a moss object (Table 4). Only NDGI, which accounts for the change in the greenness between 07/12/2022 and 16/01/2023 showed a greater diversity of the objects with the highest NDGI value = 1. The objects with NDGI=1 are P5 (rock), P67 (Wet sand), P2 (Mud), P6 (Soil on scree), P52 (Wet snow), and P50 (Muddy water) (Table 5, 6). These results show that new vegetation has developed in all these places.

Table 4 Optical indices values for mosses, lichens, and herbaceous vegetation

Index	Moss and Lichens							Herbaceous vegetation		
	P62	P61	P59	P58	P54	P45	Mean	P48	P47	Mean
MCARI2	0.13	0.16	0.04	0.1	0.09	0.05	0.09	0.07	0.02	0.04
MSAVI2	0.13	0.16	0.05	0.09	0.07	0	0.08	0.01	-0.07	-0.03
NDVI	0.07	0.08	0.02	0.05	0.04	0	0.04	0.01	-0.03	-0.01
NDWI	0.54	0.54	0.52	0.52	0.5	0.46	0.51	0.46	0.42	0.44
MSI	0.63	0.62	0.62	0.61	0.63	0.67	0.63	0.66	0.61	0.64
DI	-0.25	-0.35	-0.02	-0.18	-0.08	0.1	-0.13	0.05	0.04	0.05
NDGI	0.01	-0.1	-1	-0.88	-0.94	0.8	-0.35	0.92	0.86	0.89

Table 5 Optical indices values for water, wet snow, and glacier

Index	Glacier	Snow	Water				
	P65	P52	P50	P49	P42	P1	Mean
MCARI2	0.08	0.04	0.04	0.07	0.00	0.07	0.05
MSAVI2	0.08	0.02	0.02	0.01	-0.06	-0.01	-0.01
NDVI	0.04	0.01	0.01	0.01	-0.03	-0.01	0.00
NDWI	0.52	0.48	0.48	0.46	0.43	0.25	0.41
MSI	0.62	0.62	0.62	0.66	0.61	0.91	0.70
DI	-0.15	-0.03	-0.03	0.05	0.06	-0.11	-0.01
NDGI	0.25	1.00	1.00	0.92	0.53	0.61	0.77

Table 6 Optical indices values for sand, soil, scree, and rock

Index	Sand				Soil			Scree	Rock
	P5	P69	P67	Mean	P2	P64	Mean	P6	P51
MCARI2	0.01	0.02	0.02	0.01	0.04	0.09	0.07	0.02	0.05
MSAVI2	-0.06	-0.35	-0.07	-0.16	-0.04	0.09	0.03	-0.07	0.03
NDVI	-0.03	-0.02	-0.03	-0.03	-0.02	0.05	0.02	-0.04	0.01
NDWI	0.27	0.41	0.38	0.35	0.25	0.51	0.38	0.25	0.48
MSI	0.86	0.66	0.66	0.73	0.89	0.63	0.76	0.89	0.62
DI	-0.06	-0.26	-0.22	-0.18	-0.09	-0.23	-0.16	-0.06	-0.04
NDGI	1.00	0.46	1.00	0.82	1.00	0.03	0.52	1.00	0.53

Dynamics and territorial distribution of the radar coefficients throughout the study area

Composite radar images from one, two, or more dates were used in pseudocolors to detect wet snow, ice, water, vegetation, and rocks. The results clearly showed that locations of water, wet snow, ice and its melting can be mapped using SAR data. The same applies to vegetation such as mosses and lichens, but with a more detailed classification of radar indices. Based on the spatial distributions of the SR, it can be assumed that the data are suitable for tracking the dynamics of objects even in polar latitudes. SAR images in dB (decibels) are suitable for detecting water, wet snow and ice, as precise levels of their values can be determined. It is more complicated to use them for snow with less water content, but such objects have been successfully observed by optical indices developed for snow and ice monitoring such

as NDSI. Promising results for snow and ice monitoring showed also the DI and the NDWI. However, more experiments are needed to confirm their potential in monitoring such objects.

After processing and creating composite images, the pixel size at SAR is 12.05/16.35 m and is preserved. This is a good enough resolution to follow the general dynamics of objects, and by transforming the SAR images into decibels, an even greater logarithmic accuracy was achieved where there are already proven threshold values of water, snow, and ice. The values in the range 22-24 indicates wet snow, those in the range 25-27 indicates snow, and above 27 are the values representative for ice (Figure 13)^{3,4}.

Within the framework of the conducted research, a trend is clearly observed in the change of the land cover state and in the areas occupied by ice and snow, which is also characteristic of the seasonal dynamics.

SR values showing the change between two images close to 2.0 and above 2.0 (Figure 14) indicate that a change has occurred through the appearance or absence of a new object. Figure 14 presents the changes that occurred in the period between 29/11/2022 and 23/12/2022 (the latter date is from the synchronous experiment). Values are high in the coastal area and for water bodies, which is typical for the season and ice soup movement. For the second period of observation (11/12/2022 – 16/01/2023), a change is observed, which, according to the values of 1.7, indicates moderate changes.

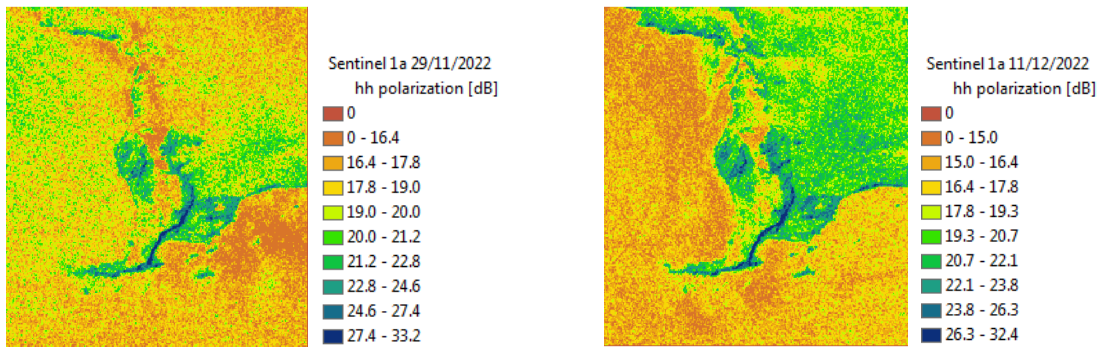


Figure 13 SAR images of study area (HH polarization) in decibels (dB) values

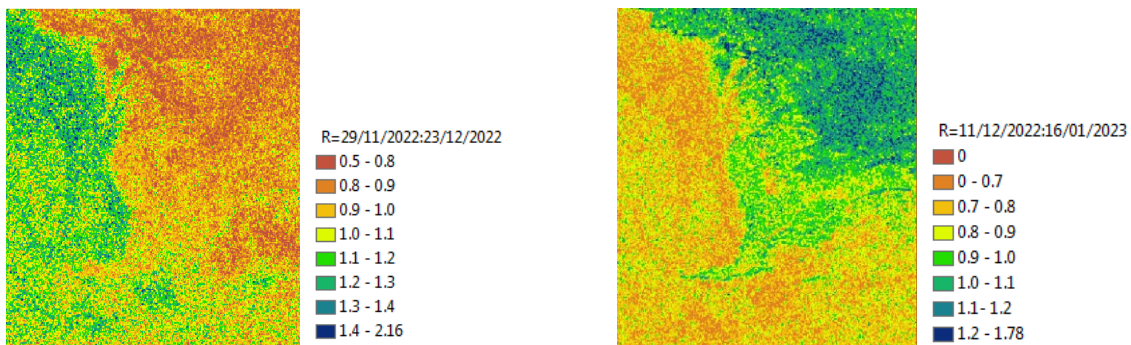


Figure 14 Spatial distribution of SAR index values throughout the study area

Automatic recording weather station (AWG)

Test data of the eco-friendly battery has shown that it works successfully in polar conditions. As an ecological source of energy, it works from 11/12/2022 until the base closes at the end of the season for the 31st Antarctic Expedition in early March. It is yet to be reinstalled and analyzed, but at this first stage, it has shown that it can run on salt water, which is a renewable energy source. The battery is an absolutely harmless source of energy, as it contains Magnesium. The data

from the AWG established the operability of the ecological magnesia-air electrochemical system for real-world operation in Antarctica.

Data generated by AWG are still being processed and analysed at this stage. The results will be published in future articles. However, energy was produced in three battery cells, which shows that this system could be successfully applied under polar conditions or in the marine environment. The energy is generated in W (Watt). In one of the cells, the voltage throughout the test reaches values above 3. The geographical coordinates and temperatures in F (Fahrenheit) table were correctly reported (Table 2).

5. CONCLUSION

The validation of the results was facilitated by the synchronized aerospace observations of the studied objects and ground-based measurements of their SRC. The specific procedures for conducting field spectrometric measurements of objects in polar conditions have been defined. Appropriate spectrometric equipment has been selected to carry out the corresponding field measurements of the Hannah Point objects. A database of primary spectral measurements was generated for the sites on 12/12/2022 and 24/12/2022. Primary spectral measurements were pre-processed for all sites, at which ground points were taken and drone photography was performed. As a result of this approach, the spectral coefficients of SR of the studied objects were obtained. After analysis of the results, a database of the SRC (spectral library) of the studied objects was created.

Several statements can be summarized as a conclusion:

1. There is an inverse relationship between color and color temperature value. The darker the object, the higher the value of the color temperature, measured in Kelvin. It is also a guarantee that the studies at high temperature values are done only in the daylight and in clear weather.
2. Sentinel-2 data can be used to locate the presence or absence of water, wet snow, snow and ice, lichens, and mosses. Optical images have a lower temporal resolution, making them less suitable for monitoring, but extremely accurate for analysis by optical indices when there is no cloud cover. In the absence of optical images, available SAR images with detailed classification can also be used to calculate indices and track changes in synchronous and asynchronous approaches. In this type of monitoring, drone data is only needed for verification and could not be mandatory. It is enough to have GCP that can be used permanently and become a permanent publicly available database structured and described by DCAT_AP for reuse.
3. The successful operation of the AWG under the Antarctic conditions is a promising sign for its deployment in various environments for monitoring not only the Antarctic, but oceans, seas, maritime transport, infrastructure, and others. The AWG is a cost-effective system with environmental focus and energy efficiency. The use of such a type of product support the sustainable development and the free exchange of data. This type of product has been successfully developed to operate on board the spacecraft systems of the European Space Agency (ESA) and NASA or to help develop a ubiquitous monitoring station to reduce the interpolation of climate data.

In general, this type of research aims to fully share its results as Open Science, to find even greater added value in reusing the data as Open Data, and to support the development and implementation of a digital space for polar data Destination Earth Antarctica following the example of the European initiative Destination Earth. The study will fully adhere to the application of the so-called FAIR principles for open and scientific data, making them Findable, Accessible, Interoperable, and Reusable.

Acknowledgements

This study was supported by „Polar scientific research for young scientists“, 2022 Bulgaria and Bulgarian Antarctic Institute (BAI)[†], contract No. 70-25-59/10.08.2022, Project: DESTINATION EARTH ANTARCTICA – DIGITAL DATA SPACE, PILOT PROJECT. Special thanks to BAI and the logistical support provided during the 31st Bulgarian Antarctic Expedition, in which our team also took part in the First Group. Special thanks to the team <https://oxymet.eu/> behind the creation of the innovative automatic recording weather station (AWG), which successfully operates in polar conditions.

REFERENCES

- [1] Mardirossian, G. [Fundamentals of Remote Aerospace Technology], New Bulgarian University, Sofia, (2015). (in Bulgarian).
- [2] Mardirossian, G. [Natural ecocatastrophes and aerospace techniques and instrumentation for their study], Prof. Marin Drinov. Academic Publishing House, Sofia, (2000). (in Bulgarian).
- [3] Gochev, D., Nedkov, R., Dimitrova, M., Trenchev, P., "Using radar imaging to study water phase transition in a circumpolar region," Proceedings SES2017, Space Research Technology Institute - Bulgarian Academy of Sciences, 201-208, (2017). ISSN: 1313-3888.
- [4] Dimitrova, M., Gochev, D. Trenchev, P., "Seasonal Changes in radar data for objects with different frozen stage obtained from Sentinel 1 data," Ecological engineering and environment protection,3, 23-28, (2017).
- [5] Alexandrov, C., Tsvetkov, M., Kolev, N., Sivkov, Y., Hristov, A., "Sentinel - 1 SAR image processing for target detection and evaluation by using Bulgarian VTMISS," 16th Conference on Electrical Machines, Drives and Power Systems, ELMA 2019 - Proceedings, 8771549, (2019).
- [6] Ivanova I., Stankova N., "Floating reed island dynamics in Srebarna Lake for spring / summer 2017 studying period using SAR data," Thirteenth Scientific Conference with International Participation, Space, Ecology, Safety, 2-4 November, Sofia, Bulgaria, 269-274, (2017).
- [7] Ivanova I., Nedkov R., Borisova D., Stankova N., "Using SAR and optical data from Sentinel satellites for precise modeling of seasonal floating reed islands dynamics in Srebarna Lake," Proc. SPIE 10790, Earth Resources and Environmental Remote Sensing/GIS Applications IX, 10790, SPIE, 107900E-1-107900E-7, (2018). DOI:10.1117/12.2325703.
- [8] Kolev, N., Sivkov, J., Tsvetkov, M., Alexandrov, C., "K band radar drone signatures measurement and simulation," Proceedings of the European Conference on Synthetic Aperture Radar, EUSAR, 2022-July, 740-745, (2022).
- [9] Tsvetkov, M.Y., "An approach for determination of sea surface plastic waste transport routes using Copernicus Marine Service products," Proceedings of SPIE, The International Society for Optical Engineering, 12268, 1226808, (2022).
- [10] Tsvetkov, M., Kolev, N., Hristov, A., Alexandrov, C., "AIS assisted Sentinel-1 SLC image ship detection, motion and displacement estimation," Proceedings of the European Conference on Synthetic Aperture Radar, EUSAR, 2021-March, 335-339, (2021).
- [11] Alexandrov, C., Kolev, N., Sivkov, Y., Hristov, A., Tsvetkov, M., "Oil spills detection on sea surface by using Sentinel-1 SAR images," 21st International Symposium on Electrical Apparatus and Technologies, SIELA 2020 - Proceedings, 9167148, (2020).
- [12] Alexandrov, C., Kolev, N., Sivkov, Y., Hristov, A., Tsvetkov, M., "Sentinel-1 SAR images of inland waterways traffic," 20th International Symposium on Electrical Apparatus and Technologies, SIELA 2018 - Proceedings, 8447125, (2018).
- [13] Avetisyan, D., Velizarova, E., Nedkov, R., "Tracing Dynamics of Relative Volumetric Soil Moisture Content Using SAR Data," Proc. SPIE. 10444, Fifth International Conference on Remote Sensing and Geoinformation of the Environment (RSCy2017), SPIE, 10444, 1044410-1-1044410-10, (2017). DOI:10.1117/12.2277506
- [14] Spasova, T., "Using radar data for monitoring flooded areas," SES 2017-Thirteenth International Scientific Conference Space, Ecology, Safety, November 2017, Sofia, Bulgaria, (2017).
- [15] Dancheva, A., Nedkov, R., Borisova, D., Spasova, T., "Using optical and radar images to study the thermal pollution from the waste disposal site around Vidin area," Proceedings of SPIE 11149, 1114928, (2019). <https://doi.org/10.1117/12.2538116>
- [16] Spasova T., Nedkov, R., "Monitoring of short-lived snow coverage by radar and optical data from Sentinel-1 and Sentinel-2 satellites", Ecological engineering and environment protection, 2, 13-19, (2017). ISSN 1311-8668.
- [17] Spasova, T., "Monitoring of short-lived snow coverage by SAR data around Livingston Island, South Shetland Islands in Antarctica, adaptation futures 2018," 5th International Climate Change Adaptation Conference, Cape Town, South Africa, 18-21 June 2018, (2018). <https://doi.org/10.15641/0-7992-2543-3>
- [18] Spasova, T., Ivanova, I., Gotchev, D., Stankova, N., "Monitoring of short-lived snow coverage based on aerospace data on Svalbard in Norway," Proceedings of SES2018, Space Research and Technology Institute - Bulgarian Academy of Sciences, (2018).
- [19] Spasova, T., Nedkov, R., Dancheva, A., Stoyanov, A., Ivanova, I., Georgiev, N., "Seasonal Assessment of the Dynamics of Sea Ice Based on Aerospace Data on Livingston Island, New Shetland Islands in Antarctica and Longyearbyen in the Arctic," Proc. SPIE 11524, Eighth International Conference on Remote Sensing and Geoinformation of the Environment (Rscy2020), 115240j (26 August 2020), (2020). Doi.Org/10.1117/12.2570829
- [20] Ivanova I., Nedkov R., Stankova N., "Studying the process of vegetation in Poda Protected Area using aerospace data," Proceedings of the Fifth International Conference "Ecological Engineering and Environment Protection" (EEEP'2017) Plovdiv, June 5-7, 191-200, (2017).
- [21] Stoyanov, A., "Application of Tasseled Cap Transformation of Sentinel-2—MSI Data for Forest Monitoring and Change Detection on Territory of Natural Park "BLUE STONES," Environmental Sciences Proceedings, 22, 1, MDPI, (2022), DOI:10.3390/IECF2022-13073, 42-1-42-6
- [22] Stoyanov, A., Borisova, D., "Monitoring on forest ecosystems by using space temporal analysis of different types aerospace data," Ecological Engineering and Environment Protection, 2, 31-37, (2017).
- [23] Lyubenova, M., Nedkov, R., Ivanova, I., Chikalanov, Al., Georgieva, N., Lyubenova, V., "Space Models of Oak Vegetation Dynamics in Protected Zone, Bulgaria," Indian Journal of Applied Research, 4 (7), 23-29, (2014), DOI:10.15373/2249555X/July2014/7,

- [24] Stankova N., Nedkov R., Ivanova I., Avetisyan D., "Modeling of forest ecosystems recovery after fire based on orthogonalization of multispectral satellite data," Proc. SPIE 10790, Earth Resources and Environmental Remote Sensing/GIS Applications IX, SPIE 10790, 107901R-1-107901R-7, (2018) .DOI:10.1117/12.2325643.
- [25] Ivanova, I., Stankova, N., Zaharinova, M., "Seasonal monitoring of Durankulak Lake using Sentinel 2 Data," Proceedings of 2nd National Workshop with International Participation on EU Copernicus Programme, 16-24, (2021). DOI:<https://doi.org/10.5281/zenodo.6497337>
- [26] Avetisyan, D., Cvetanova, G., "Assessment of drought impact on phenological development of selected sunflower hybrids based on vegetation indices and orthogonalization of multispectral satellite data," Bulg. J. Agric. Sci., 28 (6), 1006–1026, (2022).
- [27] Avetisyan, D., "A satellite-based modified plant senescence reflectance index for green-water drought monitoring," Proc. SPIE 11863, Earth Resources and Environmental Remote Sensing/GIS Applications XII, 1186318, 1186318-1-1186318-11, (2021), DOI:doi.org/10.1117/12.2599676.
- [28] Healey, S., Cohen, W., Yang, Z., Krankina, O., "Comparison of Tasseled Cap-based Landsat data structures for use in forest disturbance detection," Remote Sensing of Environment, 97, 301–310, (2005). doi: <http://dx.doi.org/10.1016/j.rse.2005.05.009>.
- [29] Avetisyan, D., Velizarova, E., Filchev, L., "Post-Fire Forest Vegetation State Monitoring through Satellite Remote Sensing and In Situ Data," Remote Sens., 14, 6266, (2022). <https://doi.org/10.3390/rs14246266>
- [30] Lapteva, G., "Hannah Point", <<https://www.gerganalapteva.com/1041108310861075/-hannah-point>>, (03 April 2023)
- [31] Bulgarian Antarctic Institute, <<https://bai-bg.weebly.com/10601083108610881072.html>>, (03 April 2023)
- [32] Copernicus Open Access Hub, <<https://scihub.copernicus.eu>>, (03 April 2023)
- [33] Sentinel Online. Sentinel-2 MSI User Guide, <<https://sentinel.esa.int/web/sentinel/userguides/sentinel-2-msi>>, (03 April 2023)
- [34] European Commission. DCAT Application Profile for data portals in Europe, <<https://joinup.ec.europa.eu/collection/semantic-interoperability-community-semic/solution/dcat-application-profile-data-portals-europe/release/11>>, (03 April 2023)
- [35] SEKONIC. Sekonic C-800-U SPECTROMETER, <<https://sekonic.com/sekonic-c-800-u-spectrometer>>, (03 April 2023)
- [36] Seconic Spectrometer. C-800 C-800-U Operating Manual, <<http://images.salsify.com/image/upload/s--8rCKPKQ5--/o69ts95u0n6rb74rds2.pdf>>, (03 April 2023)
- [37] Sentinel Online. Sentinel-1 SAR User Guide, <<https://sentinel.esa.int/web/sentinel/user-guides/sentinel-1-sar>>, (03 April 2023)
- [38] OXYMET, <<https://oxymet.eu/>>, (03 April 2023)
- [39] Borisova, D., Hristova, V., Dimitrov, V., "Thematic spectral library for remote sensing monitoring of land covers in local scale", Proc. SPIE 11534, Earth Resources and Environmental Remote Sensing/GIS Applications XI, 1153408 (20 September 2020), (2020). ; <https://doi.org/10.1117/12.2573378>
- [40] Rouse, W., Haas, R. H., Schell, J. A., Deering, D. W., "Monitoring vegetation systems in the Great Plains with ERTS," Proceedings of the Third Earth Resources Technology Satellite - 1 Symposium, 30 -317, (1974).
- [41] Qi, J., Chehbouni, A., Huete, A. R., Kerr, Y. H., Sorooshian, S., "A Modified Soil Adjusted Vegetation Index," Remote Sensing of Environment, 48, 119-126, (1994).
- [42] Haboudane, D., Miller, J. R., Pattey, E., Zarco-Tejada, P. J., Strachan, I. B., "Hyperspectral vegetation indices and novel algorithms for predicting green LAI of crop canopies: Modeling and validation in the context of precision agriculture," Remote Sensing of Environment, 90, 337-352, (2004).
- [43] Gao, B., "NDWI – A Normalized Difference Water Index for Remote Sensing of Vegetation Liquid Water from Space," Remote Sensing of Environment, 58 (3), 257 – 266, (1996).
- [44] Hunt, Jr E.R., Rock, B.N., "Detection of changes in leaf water content using Near- and Middle-Infrared reflectances," Remote Sens. Environ., 30, 43-54, (1989).
- [45] Nedkov, R., "Normalized differential greenness index for vegetation dynamics assessment," Comptes Rendus L'acad'emie Bulg. Des Sci., 70, 1143–1146, (2017).
- [46] Valovcin, F. R., "Snow/cloud discrimination," AFGL-TR-76-0174, ADA 032385, (1976).
- [47] Valovcin, F. R., "Spectral radiance of snow and clouds in the near infrared spectral region," AFGL-TR-78-0289, ADA 063761,(1978).
- [48] Kauth, R., Thomas, G., "The Tasseled Cap – a graphic description of the spectral – temporal development of agricultural crops as seen by Landsat," Proceedings Second Ann. Symp. Machine Processing of Remotely Sensed Data, West Lafayette' Purdue University Lab. App. Remote Sensing, (1976).
- [49] Crist, E., Cicone, R., "A physically-based transformation of Thematic Mapper data – the TM Tasseled Cap," IEEE Transactions on Geoscience and Remote Sensing, 22, 256 – 263, (1984). doi:<http://dx.doi.org/10.1109/TGRS.1984.350619>.
- [50] Nedkov, R., "Orthogonal Transformation of Segmented Images from the Satellite Sentinel-2," Comptes Rendus Acad. Bulg. Sci., 70, 687–692, (2017).
- [51] Crist, E., Kauth, R., "The Tasseled Cap de-mystified," Photogrammetric Engineering and Remote Sensing, 52, 81 – 86, (1986).